Observational Assessment of Nonlocal Heat Flux Feedback in the North Atlantic by GEFA

NA WEN

Key Laboratory of Meteorological Disaster, Ministry of Education, and College of Atmospheric Sciences, Nanjing University of Information Science and Technology, Nanjing, China

ZHENGYU LIU

Center for Climate Research, University of Wisconsin—Madison, Madison, Wisconsin

QINYU LIU

Physical Oceanography Laboratory and College of Physical and Environmental Oceanography, Ocean University of China, Qingdao, China

(Manuscript received 8 December 2011, in final form 16 August 2012)

ABSTRACT

Most previous studies have proven the local negative heat flux feedback (the surface heat flux response to SST anomalies) in the midlatitude areas. However, it is uncertain whether a nonlocal heat flux feedback can be observed. In this paper, the generalized equilibrium feedback assessment (GEFA) method is employed to examine the full surface turbulent heat flux response to SST in the North Atlantic Ocean using NCEP–NCAR reanalysis data. The results not only confirm the dominant local negative feedback, but also indicate a robust nonlocal positive feedback of the Gulf Stream Extension (GSE) SST to the downstream heat flux in the subpolar region. This nonlocal feedback presents a strong seasonality, with response magnitudes of 16 W m^{-2} K^{-1} in winter and 1.2 W m^{-2} K^{-1} in summer. Further study indicates that the nonlocal effect is initiated by the adjustments of the downstream surface wind to the GSE SST anomalies.

1. Introduction

The boundary interaction of the surface heat flux with the sea surface temperature (SST) holds the key to understanding the nature of the coupled atmosphere–ocean system. Dominant heat flux forcing has been well established by both observations and numerical models (Kushnir et al. 2002). However, our current understanding of the surface heat flux feedback—the surface heat flux response to the SST anomalies—remains limited. Because of the causality problem, the heat flux response to the SST is difficult to observe, especially in midlatitude regions with strong atmospheric internal variability. To study this problem, ensemble model experiments that suppress the atmospheric internal variability have been widely performed. However, the results are strongly dependent on the specific model employed. Some studies have shown a negative feedback (Rahmstorf and Willebrand 1995; Kushnir and Held 1996), whereas others have reported a positive feedback (Latif and Barnett 1994; Peng et al. 1995). These controversial results require an observational benchmark for calibrating model performance.

Frankignoul et al. (1998) proposed a statistical method [hereinafter termed equilibrium feedback assessment (EFA)] for separating the ocean forcing signal from the atmospheric internal variability. The method was applied in an observational study of the surface heat flux feedback over the eastern and central North Atlantic, where the ocean current is weak and the local response assumption is reasonable (Frankignoul et al. 1998). The study revealed a local negative feedback with an amplitude of approximately 20 W m^{-2} K^{-1}. Their succeeding studies (Frankignoul and Kestenare 2002; Frankignoul et al. 2002; Park et al. 2005) further confirmed the

Corresponding author address: Dr. Na Wen, College of Atmospheric Science, Nanjing University of Information Science and Technology, Nanjing 210044, China.
E-mail: wenna@nuist.edu.cn

DOI: 10.1175/JAMC-D-11-0257.1

dominant local negative response of the heat flux to the SST in both the North Pacific and North Atlantic Oceans. As the main component of the surface heat flux, the turbulent heat flux exerts a local negative feedback over most ocean basins (Tanimoto et al. 2003; Wen et al. 2005).

In addition to the dominant local feedback, a nonlocal feedback response of the heat flux to the SST may also occur. As recognized by Palmer and Sun (1985), the atmospheric response to the warm SST anomaly of the Gulf Stream Extension (GSE) region is a downstream ridge response in the central North Atlantic. The results of their model diagnostic indicated that transient eddy activity plays an important role in tilting the atmospheric response to the upstream SST anomaly. The downstream warm SST-ridge response is also identified from the observations of Ciasto and Thompson (2004). They found a significant impaction of the wintertime SST anomalies over the GSE region on the Northern Hemisphere annular mode on intraseasonal time scales. Similarly, Liu and Wu (2004) reported a downstream warm SST-ridge response of the atmosphere over the Aleutian Islands to the Kuroshio Extension SST anomaly, based on their coupled GCM experiment. In addition to these studies, many others have shown that the SST anomalies over the North Hemisphere western boundary current region play an important role in large-scale atmosphere–ocean interaction (Czaja and Frankignoul 2002; Liu et al. 2006; Frankignoul and Sennechael 2007; Minobe et al. 2008; Kwon et al. 2010). In general, a nonlocal atmospheric response would facilitate the underlying boundary air–sea interaction and result in the heat flux nonlocal feedback. In addition to the atmospheric dynamic adjustments, the ocean advection could also add to the nonlocal heat flux feedback to the underlying SST anomalies, such as in Gulf Stream region where the current is strong. The heat advection can induce the variation of the heat content and heat storage in the vicinity of the current region, and then modify the SST variability there on interannual and longer time scales. The nonlocal SST anomalies may re-form the local heat flux feedback in these areas and result in the interannual-to-decadal climate variations (Kelly and Dong 2004). Therefore, it is more plausible that a nonlocal heat flux feedback may be observable.

However, it is a challenge to separate the nonlocal from the local feedback using this technique, because of the complex interferences from the interrelated SST forcings. The conventional approach to find the SST influence in a given region is to filter out the dominant external forcing with regression and then to assess the climate impacts using the residual variability, such as removing the ENSO signal to study midlatitude air–sea interaction (Vimont et al. 2001; Alexander et al. 2002; Zhong and Liu 2008). But, this approach is effective only if there is a single dominant external forcing and the forcing is known a priori. In general, atmospheric anomalies might be influenced by multiple ocean forcings that interact with each other in a complex way (Lau et al. 2006). To address this problem, Liu et al. (2008, hereafter LWL) generalize the EFA method from the univariate ocean forcing into the multiple ocean forcings, using the generalized equilibrium feedback assessment (GEFA), to exclusively identify the impact of each SST forcing. Unlike EFA, GEFA can automatically separate each contribution of the regional SST to the atmosphere from the interrelated SST forcings, without any prefiltering. The GEFA method has been applied to distinguish the atmospheric geopotential height response to global SST variability modes (Wen et al. 2010), and to evaluate the attribution of the regional SST variability modes to the U.S. precipitation variability (Zhong et al. 2011). Their studies serve as a demonstration of the potential utility of GEFA in identifying multiple surface feedbacks to the atmosphere in observations.

In this paper, we aim to detect the nonlocal heat flux feedback in the North Atlantic from the observations. The GEFA method is employed to do the investigation. The results show a robust nonlocal positive feedback of the GSE SST to the downstream heat flux in the subpolar region. The paper is organized as follows. In section 2, the data and methods are introduced. A nonlocal response is identified for a three-region case in section 3, which is then further confirmed in an extended six-region case in section 4. The last section summarizes the main points of this study.

2. Data and methods

The data used for the study come from the National Centers for Environmental Prediction–National Center for Atmospheric Research (NCEP–NCAR) reanalysis (Kalnay et al. 1996). The variables include the surface turbulent heat flux (where the downward direction is positive), SST, sea level pressure, and sea surface wind on a T62 Gaussian grid. The domain investigated is 20°–60°N, 80°W–0°, covering the North Atlantic basin. In terms of the largest SST variability in the basin (Fig. 1a), the North Atlantic is divided into three regions: the first region is located at the GSE (35°–55°N, 60°–30°W), the second lies in the subpolar region (40°–60°N, 25°–5°W), and the third is in the subtropic region (20°–35°N, 40°–15°W). Monthly data over the period 1958–2011 were anomalies from their seasonal cycle and detrended with a third-order polynomial filter before the analysis.

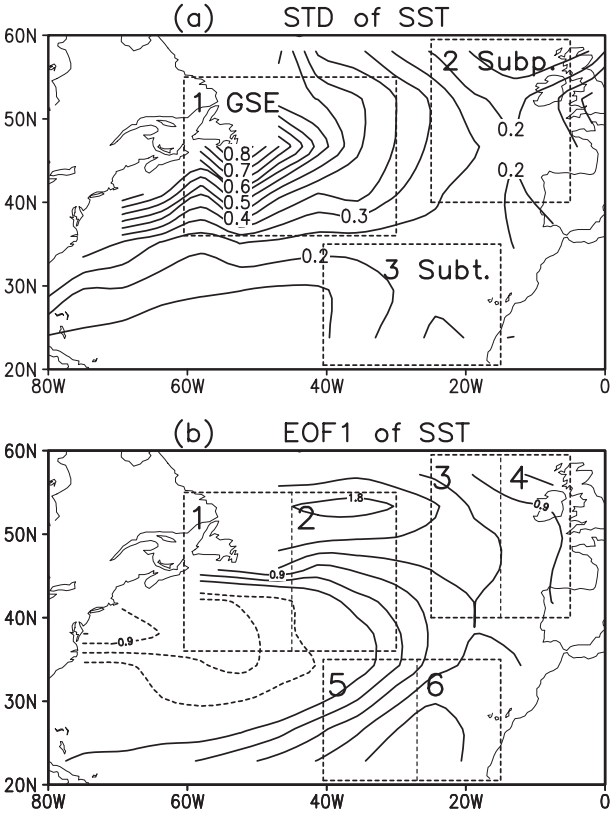

FIG. 1. (a) Standard deviation of the monthly SST (°C) from the NCEP–NCAR reanalysis data for 1958–2011. The three regions studied in section 3 are marked, where the regions 1, 2, and 3 correspond to the GSE and the subpolar and subtropic regions, respectively. (b) The pattern of the first EOF of the SST. The above three regions are further subdivided into six regions, as marked (see section 4).

To detect the nonlocal heat flux feedback in the North Atlantic, the GEFA method was used. The technique is superior at identifying the impact of each SST forcing within a unified framework. It generalizes the EFA's univariate ocean forcing as multivariate ocean forcings, such that the quasi-equilibrium heat flux equation is expressed as

$$x_i(t) = (b_{i1} \quad b_{i2} \quad \cdots \quad b_{ij}) \begin{bmatrix} y_1(t) \\ y_2(t) \\ \vdots \\ y_j(t) \end{bmatrix} + n_i(t). \qquad (2.1)$$

Its vector form is

$$\mathbf{x}(t) = \mathbf{B}\mathbf{y}(t) + \mathbf{n}(t), \qquad (2.2)$$

where $\mathbf{x}(t)$ is the surface turbulent heat flux, $\mathbf{y}(t)$ is the variable of SST with $\mathbf{B}$ as the full feedback matrix, and $\mathbf{n}(t)$ is the atmospheric internal variability. Matrix $\mathbf{B}$ includes all the feedback information between the entire SST field and the heat flux field, with b_{ij} representing the atmospheric heat flux response of the ith region $x_i(t)$ to the individual SST forcing at the jth region $y_j(t)$. Taking advantage of the fact that the leading ocean cannot be forced by the lagging atmosphere, the GEFA estimation of the full feedback matrix $\mathbf{B}$ can be derived after multiplying the transposed leading SST $\mathbf{y}^{\mathrm{T}}(t-\tau)$ as

$$\mathbf{B}(\tau) = \mathbf{C}_{xy}(\tau)\mathbf{C}_{yy}^{-1}(\tau), \quad \tau > \tau_n, \qquad (2.3)$$

with the sampling error

$$\varepsilon(\tau) = \mathbf{C}_{ny}(\tau)\mathbf{C}_{yy}^{-1}(\tau). \qquad (2.4)$$

Here, τ is a lag time longer than the persistent time of the atmospheric internal variability τ_n (τ is taken to be 1 month in this calculation), and $\mathbf{C}_{\mathbf{uv}}(\tau) = \mathbf{u}(t)\mathbf{v}'(t-\tau)/T$ represents a lagged covariance matrix with T as the sample size. For seasonal GEFA estimation, the data from three consecutive monthly anomalies are used to increase the realization numbers and thus reduce the sampling error (Liu et al. 2012a,b). Taking the summer feedback as an example, the matrix $\mathbf{B}$ during June–August is calculated by using the leading SST during May–July in Eq. (2.3). The winter (December–February) feedback matrix $\mathbf{B}$ is calculated similarly.

One thing worth mentioning is that when using GEFA, the sampling error would be rapidly amplified with the increase in spatial resolution, as discussed in LWL. This is because the covarying SST makes the covariance matrix $\mathbf{C}_{yy}(\tau)$ in Eq. (2.4) singular and thus produces a large sampling error. To optimize the GEFA estimation, an empirical method—the truncated empirical orthogonal function (EOF) method—was introduced (LWL; Fan et al. 2011). Through the reconstruction of SST anomalies using the leading EOF modes, this approach reduces the forcing field noise and, in turn, the sampling error. In this paper, the truncated EOF method is used in a six-region case to check the stability of the nonlocal feedback of the GSE SST on the downstream heat flux.

In addition, the univariate EFA estimation (Frankignoul et al. 1998) of the heat flux response to the SST is also calculated in this paper. The EFA feedback matrix $\mathbf{A}$ is denoted as

$$\mathbf{A} = (a_{ij}) \quad (i = 1, \ldots, I;\ j = 1, \ldots, J), \qquad (2.5)$$

with $a_{ij} = \langle x_i(t), y_j(t-\tau)\rangle / \langle y_j(t), y_j(t-\tau)\rangle$ and $\tau > \tau_n$, (2.6)

TABLE 1. The annual GEFA feedback matrix **B**, EFA feedback matrix **A**, and mutual matrix **M** for the three-region case. The matrices **B**, **A**, and **M** are calculated by Eqs. (2.3), (2.6), and (2.9), respectively, using year-round data. Note that in the calculations, each row and column uses time t applied to the quantities in the columns and $t - \tau$ applied to the quantities in the header row, where the lag time τ is taken to be 1 month. The symbols H_1, H_2, and H_3 in the left column of the table indicate the heat fluxes in regions 1, 2, and 3, respectively, and T_1, T_2, and T_3 in the top row denote the SSTs in regions 1, 2, and 3, respectively. For the feedback matrices, the diagonal elements denote the local feedback, whereas the off-diagonal elements indicate the nonlocal feedback. Each column ($j = 1, 2,$ and 3) indicates the response of the heat flux in different regions to the SST anomaly of a certain region (e.g., for the first column in matrix **B**, b_{11}, b_{21}, and b_{31} denote the responses of the heat flux in regions 1, 2, and 3 to the SST anomaly in region 1, respectively). Similarly, each row ($i = 1, 2,$ and 3) shows the response of the heat flux in a certain region to the SST anomaly in different regions. In matrices **B** and **A**, negative values indicate a negative feedback and vice versa. The boldface italic values indicate the significance at the 95% confidence level, and the only boldface values are at the 90% confidence level, as tested by a Monte Carlo method in which the year of the heat flux was scrambled 1000 times. As to the mutual matrix **M**, the element m_{ij} reflects the relation between the ith region SST T_i and the jth region SST T_j. It represents the weight of the contribution (GEFA feedback) of the interrelated region SST to the total EFA feedback for the region of interest. For the significance in matrix **M**, the rule is the same as that in feedback matrices **B** and **A**.

	GEFA feedback **B**			EFA feedback **A**				Mutual matrix **M**		
	T_1	T_2	T_3	T_1	T_2	T_3		T_1	T_2	T_3
H_1	***−15***	**−6.7**	3.8	***−16***	**−6.8**	0.3	T_1	***1.0***	***0.2***	0.0
H_2	***5.5***	***−18***	0.3	1.8	***−17***	**−7.5**	T_2	***0.2***	***1.0***	***0.4***
H_3	−2.2	−2.5	***−18***	−4.1	***−15***	***−19***	T_3	0.1	***0.7***	***1.0***

and where $\langle p, q \rangle$ indicates the covariance between p and q. The matrix **A** is also called the total feedback, with a_{ij} indicating the total heat flux response of the ith region to the SST in the jth region. Its relation with the GEFA feedback matrix **B** is determined by mutual matrix $\mathbf{M} = (m_{ij})$ $(i = 1, \ldots, I; j = 1, \ldots, J)$, as

$$\mathbf{A} = \mathbf{BM}, \tag{2.7}$$

$$\text{with} \quad a_{ij} = \sum_{k=1}^{J} b_{ik} m_{kj} \quad \text{and} \tag{2.8}$$

$$m_{ij} \equiv \mathbf{C}_{y_i y_j}(\tau)/\mathbf{C}_{y_j y_j}(\tau). \tag{2.9}$$

For the total feedback matrix **A**, the total feedback a_{ij} not only includes feedback from its own region b_{ij} but also involves the influence of other regions' SST forcings weighted by m_{ij}. The mutual matrix **M** reflects the relation between the SSTs of the different regions. Generally, because of the covariance of the SST of the forcing field, the feedback matrix **B** differs from the total matrix **A**.

3. Nonlocal feedback identified in a three-region case

In the following, we apply GEFA to study the ocean–atmosphere thermal feedback over the North Atlantic. The assessment is first conducted for a simple three-region case, where the regional heat flux and the SST are denoted as $H_i (i = 1, 2,$ and 3) and $T_j (j = 1, 2,$ and 3) (the numbers 1, 2, and 3 denoting the GSE, subpolar, and subtropic regions respectively, as shown in Fig. 1a). To provide a better understanding of the GEFA estimation, the EFA result is given as well. As shown in Table 1, the annual GEFA feedback matrix **B**, the total EFA feedback matrix **A** (both: W m^{-2} K^{-1}), and the mutual matrix **M** are calculated using Eqs. (2.3), (2.6), and (2.9), respectively. It reveals the general picture of the heat flux feedback in the North Atlantic. Considering the seasonality, we further calculate the winter and summer feedbacks shown in Tables 2 and 3, respectively.

From Table 1, it is clear that the annual feedback matrix **B** is dominated by significant negative feedback along the diagonal, consistent with our understanding that the turbulent heat flux response is dominated by local negative feedback. This dominant local feedback is consistent with the estimation in the total matrix **A**, indicating the damping of the turbulent heat flux to the SST anomalies. It varies by season, with response magnitudes of approximately ~20 W m^{-2} K^{-1} in winter (see Table 2) and ~5 W m^{-2} K^{-1} in summer (see Table 3). The strong (weak) response in winter (summer) is in line with the results in Park et al. (2005). They suggested that the negative turbulent heat flux feedback mainly stems from the weak moisture–temperature adjustment of the surface air to the underlying SST anomalies. This implies that local cooling and drying responses of surface air to warm SST anomalies tend to counteract the downward surface heat flux forcing (Nonaka and Xie 2003). The physical understanding of the air–sea thermal feedback can be evidenced by the lagged regression of the surface pressure and wind on the GSE SST, especially in winter (Fig. 2b). The warm SST anomalies over the GSE region tend to induce the local offshore cold, dry surface wind and, in turn, the anomalous heat released from the ocean. Overall, the dominant local negative

TABLE 2. As in Table 1, but for the winter (December–February) GEFA feedback matrix **B**, EFA feedback matrix **A**, and mutual matrix **M**.

	GEFA feedback **B**			EFA feedback **A**				Mutual matrix **M**		
	T_1	T_2	T_3	T_1	T_2	T_3		T_1	T_2	T_3
H_1	***−28***	0.3	4.8	***−28***	0.6	3.5	T_1	***1.0***	0.1	0.1
H_2	***16***	**−19**	−4.5	**12**	***−20***	−12	T_2	***0.2***	***1.0***	***0.4***
H_3	−7.1	−5.4	−19	−9.1	**−17**	**−22**	T_3	0.1	***0.6***	***1.0***

feedback indicates that GEFA can be used to assess the full heat flux response to the SST.

Despite the dominant diagonal elements in **B**, there is a significant off-diagonal element $b_{21} = 5.5$ in Table 1, which represents a nonlocal positive feedback response of the subpolar region's heat flux to the GSE region's SST. Furthermore, the nonlocal feedback presents a strong seasonality. In winter (Table 2), its response magnitude is high, up to 16 W m^{-2} K^{-1}, which is comparable to its local response amplitude, 19 W m^{-2} K^{-1}, in the subpolar region . The winter nonlocal GEFA response is also consistent with the corresponding total feedback **A** ($a_{21} = 12$) in both sign and magnitude. As shown for the mutual matrix **M** (in Table 2), the GSE SST is only slightly correlated with the SST in the other two regions ($m_{21} = 0.2$ and $m_{31} = 0.1$) (some hints are also seen from the spatial regression of the winter SST on the GSE SST, as shaded in Fig. 2b), and therefore there is little distortion in the heat flux response to the GSE SST forcing ($a_{21} = b_{21} \times m_{11} + b_{22} \times m_{21} + b_{23} \times m_{31} \approx b_{21}$). In comparison with winter, the summer response is weak, $b_{21} = 1.2$ (in Table 3), but it is still positive and above the 90% confidence level. Physically, this remote positive feedback suggests that a warm SST anomaly over the GSE region tends to warm the downstream subpolar SST through a downward heat flux. This downstream response seems to be caused mainly by a warm SST-ridge response, as indicated by Fig. 2. The ridge response over the subpolar region, which is strong in winter (Fig. 2b) and weak in summer (Fig. 2c), reduces the westerly wind speed and, in turn, the latent and sensible heat losses in that area—more heat loss in winter and less heat loss in summer. This downstream warm SST-ridge response in the atmosphere and the associated downstream warming effect on the SST have been previously studied both in observations and climate models (e.g., Palmer and Sun 1985; Ciasto and Thompson 2004). In the North Atlantic, it is a passage of the storm track over the GSE region. The warm SST anomalies there could strengthen the SST gradient and activate the baroclinic eddies. As a result, it generates a downstream ridge response and, in turn, the nonlocal positive heat flux response in the subpolar region. Therefore, the statistic result that the robust nonlocal heat flux feedback is detected in the GSE region, rather than in the subpolar or subtropic region, is consistent with our physical understanding.

The annual total matrix **A** in Table 1 appears to show an additional significant nonlocal negative feedback, $a_{32} = -15$, implying a heat flux reduction in the subtropics in response to a warming in the subpolar region. The pattern is the same for the winter and summer total feedbacks ($a_{32} = -17$ in Table 2 and $a_{32} = -6.7$ in Table 3). This overall response, however, is not presented in the feedback matrix **B** and should therefore be interpreted with caution. Some insight can be gained by examining the mutual matrix **M**, which has a significant off-diagonal subtropical SST response to the subpolar SST, with $m_{32} = 0.7$ (see Table 1). With the equivalence relation in Eq. (2.8), we have

$$-15 = a_{32} = b_{31} \times m_{12} + b_{32} \times m_{22} + b_{33} \times m_{32}$$
$$\approx b_{33} \times m_{32} = -18 \times 0.7 = -12.6.$$

Therefore, this seemingly nonlocal total feedback does not represent a true nonlocal response of the subtropical heat flux to the subpolar SST variability b_{32}. Instead, it mainly recaptures part of the local negative response of the subtropical heat flux to the subtropical SST variability b_{33} that covaries with the subpolar SST

TABLE 3. As in Table 1, but for the summer (June–August) GEFA feedback matrix **B**, EFA feedback matrix **A**, and mutual matrix **M**.

	GEFA feedback **B**			EFA feedback **A**				Mutual matrix **M**		
	T_1	T_2	T_3	T_1	T_2	T_3		T_1	T_2	T_3
H_1	***−3.3***	**−3.7**	2.1	***−3.7***	−2.5	0.1	T_1	***1.0***	0.2	0.0
H_2	**1.2**	***−4.4***	1.3	0.6	***−3.1***	−1.1	T_2	0.1	***1.0***	***0.6***
H_3	***−2.2***	**−2.7**	***−4.4***	***−2.6***	***−6.7***	***−5.9***	T_3	0.1	***0.8***	***1.0***

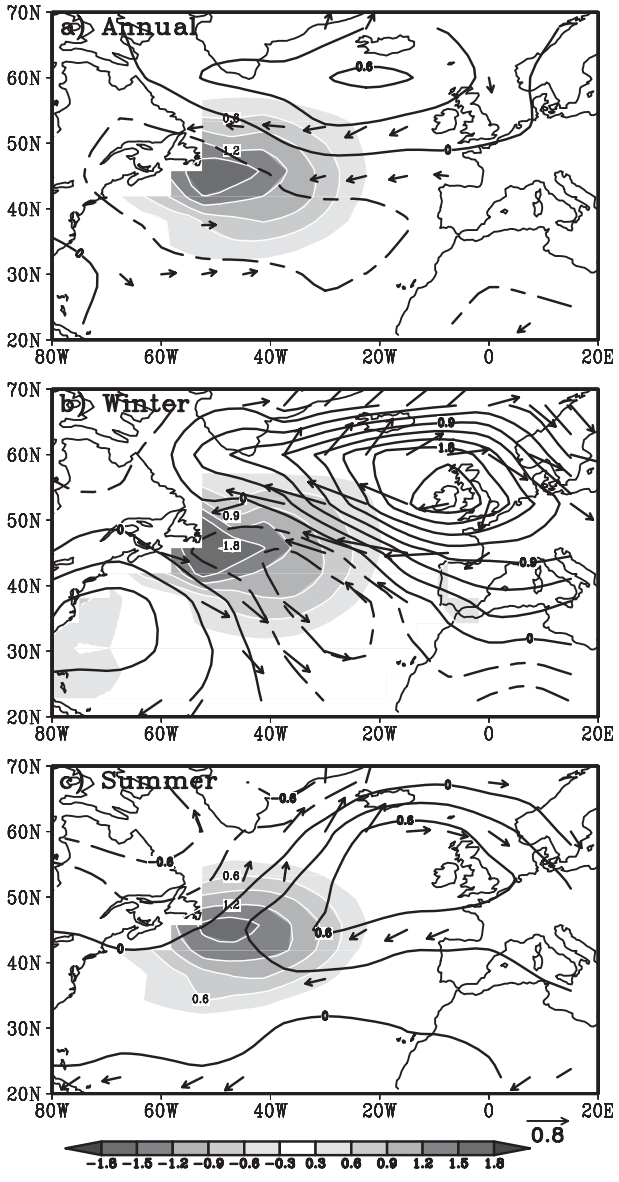

FIG. 2. Regression of the SLP [black contours; contour interval (CI) = 0.3 hPa K^{-1}] and surface winds (vectors; m s^{-1} K^{-1}) against the SST variability in the GSE region (region 1 in Fig. 1a) with the SST leading by 1 month, using (a) year-round, (b) winter, and (c) summer data, respectively. A wind vector is plotted when the correlation is statistically different from zero at the 95% level. The shading indicates the instantaneous regression of the SST onto the winter SST variability in the GSE region, with white solid (black dashed) lines for positive (negative) values (CI = 0.3).

variability m_{32}. The high positive correlation between the SSTs in the subpolar and subtropical regions is associated with the dominant tripole SST variability over the North Atlantic (such as Fig. 1b), which is predominantly forced by the spatially coherent atmospheric variability of the North Atlantic Oscillation (NAO; Cayan 1992; Deser and Timlin 1997).

In short, in the three-region case, GEFA confirms the dominant local negative feedback, and further identifies a significant nonlocal positive feedback from the GSE SST to the heat flux downstream in the subpolar region. This nonlocal effect is likely caused by the adjustments of the downstream surface wind to the SST anomalies over the GSE region.

4. Further confirmation in a six-region case

Next, we extend our analysis from three regions to a six-region case to examine the stability of the nonlocal effect of the GSE SST on the downstream heat flux. Each of the three regions is subdivided into a pair of subregions (Fig. 1b) in the east and west. The feedback matrix is estimated using the year-round data, as indicated in Tables 4–7 . Here, the seasonal feedback is not shown in the six-region case. The stability of the seasonal nonlocal feedback is the same as that of the annual feedback. And the seasonality of the nonlocal feedback in the six-region case is also consistent with that in the three-region case.

For the annual total feedback in Table 5, there is no big difference with an increased spatial resolution. Likewise, in $\mathbf{A}_6$, the local response along the diagonal is dominated by the negative feedback, with an amplitude of approximately ~20 W m^{-2} K^{-1}. Furthermore, each pair of subregions exhibits a strong negative feedback on each other (a_{21} and a_{12}, a_{43} and a_{34}, and a_{65} and a_{56}) because of their proximity. The remote positive feedback of the GSE SST to the downstream subpolar heat flux is now dominated by the response of the eastern (western) subpolar subregion to the eastern (western) GSE subregion (a_{31} and a_{42}). In addition, the remote negative total feedback of the subpolar SST to the subtropical heat flux is now dominated by that from both subpolar subregions to both subtropical subregions (a_{53}, a_{54}, a_{63}, and a_{64}).

In contrast, the annual feedback matrix $\mathbf{B}_6$ (in Table 4) exhibits an amount of noise, as seen from the less clear diagonal dominance and the large far-off-diagonal elements. This finding is expected from the simple model study in LWL, due to the enhanced resolution and, in turn, the enhanced sampling error. Each pair of subregions is neighboring each other, and therefore their SSTs tend to covary with each other, as shown in the near-diagonal elements in $\mathbf{M}_6$ (in Table 6). This covariability increases the singularity of the lagged SST covariance matrix $\mathbf{C}_{yy}(\tau)$ in Eq. (2.4) and, as a result, produces a sampling error in $\mathbf{B}_6$.

Following the simple model study in LWL, the sampling error in $\mathbf{B}_6$ can be reduced by truncating the SST EOF mode. The total matrix $\mathbf{A}$ seems to be insensitive to

TABLE 4. As in Table 1, but for the annual GEFA feedback matrix $\mathbf{B}_6$ for the six-region case. The subscript of $\mathbf{B}_6$ represents the number of the leading SST EOF modes retained for the reconstruction of the SST anomalies. Here, the number 6 indicates the full information of the SST forcing field is kept in assessment.

	GEFA feedback matrix $\mathbf{B}_6$					
	T_1	T_2	T_3	T_4	T_5	T_6
H_1	***−23***	7.7	−2.8	1.2	***−11***	***9.2***
H_2	5.8	***−20***	−5.6	−6.1	5.6	1.5
H_3	***11***	−8.6	0.0	***−21***	3.5	1.1
H_4	7.4	−9.9	***24***	***−35***	3.8	−4.0
H_5	1.2	−3.2	4.0	−7.4	**−14**	−3.4
H_6	1.0	−6.0	2.7	−3.3	−0.2	***−17***

the EOF truncation (as long as the first two leading EOFs are retained; not shown), consistent with the simple model study in LWL. In contrast, the feedback matrix shows a much greater sensitivity to the EOF truncation. Since the true $\mathbf{B}$ is unknown in the observations, we will empirically determine an optimal $\mathbf{B}$ from their successive convergences. We found that $\mathbf{B}_4$ [explained variance (EV) = 96%] or $\mathbf{B}_5$ (EV = 99%) appears to be the optimal estimator. This selection is based partly on the successive pattern correlations, $\mathrm{cor}\langle \mathbf{B}_f, \mathbf{B}_{f-1} \rangle$, which are 0.41, 0.62, 0.82, 0.83, and 0.66 for $f = 2, 3, 4, 5,$ and 6, respectively, exhibiting a maximum stability from $\mathbf{B}_4$ to $\mathbf{B}_5$ [a similar conclusion can be obtained from its amplitude ratio $\sigma(\mathbf{B}_{f-1})/\sigma(\mathbf{B}_f)$]. This optimal estimator is partly selected based on the physical interpretation of the matrix itself. Indeed, the $\mathbf{B}_4$ in Table 7 is featured by a dominant local response along the diagonal and the negative feedback between each pair of subregions around the diagonal. Additionally, $\mathbf{B}_4$ has the most significant nonlocal feedback, with a positive response of the eastern subpolar region heat flux to the eastern GSE SST anomaly b_{42}, a feature that is stable with the truncation of EOFs (not shown). This result is also consistent with the SST-lead regression of wind, which exhibits a maximum value in the eastern part of the subpolar region (as Fig. 2). Finally, similar to the three-region case, the nonlocal total feedback from the subpolar region to the subtropical region (large a_{53}, a_{54}, a_{63}, and a_{64}) disappears in $\mathbf{B}_4$ (small and insignificant b_{53}, b_{54}, b_{63}, and b_{64}), because of the covariance of the subpolar and subtropical SSTs in the mutual matrix (large m_{53}, m_{54}, m_{63}, and m_{64} in Table 6).

TABLE 6. As in Table 4, but for the annual mutual matrix $\mathbf{M}_6$ for the six-region case.

	Mutual matrix $\mathbf{M}_6$					
	T_1	T_2	T_3	T_4	T_5	T_6
H_1	***1.0***	***0.7***	0.0	0.1	0.0	0.0
H_2	***0.8***	***1.0***	***0.4***	0.0	***0.1***	0.0
H_3	0.1	***0.5***	***1.0***	***0.8***	***0.4***	***0.3***
H_4	0.0	0.1	***0.7***	***1.0***	***0.4***	***0.4***
H_5	0.0	***0.2***	***0.5***	***0.5***	***1.0***	***0.6***
H_6	0.0	0.1	***0.6***	***0.8***	***1.0***	***1.0***

Similar results were obtained in a complementary six-region analysis, in which each of the three regions in Fig. 1a was divided into a pair of subregions in the north and south. The optimal truncation seems to occur for EOF truncations of 4 (EV = 93%) and 5 (EV = 97%). The nonlocal feedback impact from the GSE region on the subpolar region occurs from both GSE subregions to the southern subpolar subregion. In addition, as the resolution is further increased, the GEFA results become even more noisy (not shown), as expected. Nevertheless, further analysis suggests some clues that are consistent with the major features found in the three- and six-region cases (not shown).

The above discussion further confirms that, besides the dominant local negative feedback in the North Atlantic, there is a robust nonlocal positive feedback of the GSE SST to the downstream heat flux in the subpolar region, specifically from the GSE region to the eastern subpolar region.

TABLE 5. As in Table 4, but for the annual EFA feedback matrix $\mathbf{A}_6$ for the six-region case.

	EFA feedback matrix $\mathbf{A}_6$					
	T_1	T_2	T_3	T_4	T_5	T_6
H_1	***−18***	***−7.4***	−1.8	−0.4	−1.4	2.2
H_2	***−9.2***	***−18***	***−15***	***−6.4***	−0.5	0.2
H_3	***4.7***	−2.9	***−17***	***−18***	***−5.9***	***−5.8***
H_4	1.9	3.8	***−6.5***	***−18***	***−6.4***	***−8.5***
H_5	−1.1	−3.5	***−11***	***−14***	***−19***	***−14***
H_6	−3.1	−5.4	***−12***	***−15***	***−18***	***−18***

TABLE 7. As in Table 4, but here the annual GEFA feedback matrix $\mathbf{B}_4$ is assessed using the reconstructed SST anomalies from the first four leading EOF modes.

	GEFA feedback matrix $\mathbf{B}_4$					
	T_1	T_2	T_3	T_4	T_5	T_6
H_1	***−17***	−0.3	***4.1***	−2.6	1.7	−0.8
H_2	2.2	***−14***	***−11***	−1.7	1.4	***4.5***
H_3	4.7	0.2	***−12***	***−11***	2.6	1.2
H_4	***−6.2***	***9.8***	−2.2	***−12***	1.5	***−3.6***
H_5	−0.4	−0.8	−1.3	−1.6	***−7.4***	***−8.9***
H_6	−2.3	−1.3	−0.8	−1.6	***−8.4***	***−10***

5. Summary

In a case study of air–sea interaction, a statistical method—the generalized equilibrium feedback assessment—was applied to the North Atlantic to assess the observed turbulent heat flux feedback. This study not only confirms the dominant local negative feedback found in the previous work, but also reports a robust nonlocal positive feedback response of the downstream heat flux in the subpolar region to the Gulf Stream Extension SST. This nonlocal feedback is strong in winter with the response amplitude up to 16 W m^{-2} K^{-1} and weak in summer with a response amplitude of 1.2 W m^{-2} K^{-1}. The nonlocal effect is likely initiated by the atmospheric dynamic adjustments. An anomalous downstream easterly surface wind in the subpolar region is induced by warm SST anomalies in the GSE region, which increases the heat flux toward the ocean, thus increasing the SST in that region.

The confirmation of the dominant local feedback indicates the ability of GEFA to assess the full heat flux response to the SST. This result strengthens our confidence in the nonlocal feedback response of the downstream heat flux to the GSE SST, which was first detected by GEFA in a three-region case and further confirmed in a six-region case. As a comparison, the univariate EFA also detected the robust nonlocal feedback during winter. This result arises because of the independence of the GSE SST from the other two regions—subpolar and subtropical. Furthermore, the EFA result showed an additional significant nonlocal negative feedback from the subpolar SST to the subtropic heat flux, which actually employs the negative local feedback of its covarying subtropic SST and therefore distorts the true feedback.

Our study was limited to the North Atlantic, which is less influenced by the El Niño–Southern Oscillation (ENSO). To highlight the findings in this paper, we also examined the GEFA estimation using data from which the ENSO signal was removed and obtained similar results. In addition, we did a sensitivity test on the location of the GSE region, moving the box in Fig. 1a to the east, west, north, and south by 5°. The main conclusion of the paper is unchanged. In this study, a truncated EOF method was used to optimize the GEFA estimation in the six-region case. However, when the spatial resolution is further increased, the empirical method does little to improve the accuracy. A more comprehensive GEFA analysis, including aspects such as EOF mode feedback (Wen et al. 2010) or singular value decomposition–optimal feedback (Liu and Wen 2008), making full use of the available data, is recommended for future work.

Acknowledgments. We thank the editor and the two anonymous reviewers for helpful and constructive comments. The author, Wen Na, thanks Prof. Klause Fraedrich and Yu Yongqiang for their useful discussion and kind English editing. This work is supported by 2012CB955200, Chinese NSF 41005048, GYHY200906016, KLME1001, and NUIST Fund 20100317.

REFERENCES

Alexander, M. A., I. Bladé, M. Newman, J. R. Lanzante, N. C. Lau, and J. D. Scott, 2002: The atmospheric bridge: The influence of ENSO teleconnections on air–sea interaction over the global oceans. *J. Climate,* **15,** 2205–2231.

Cayan, D. R., 1992: Latent and sensible heat flux anomalies over the northern oceans: Driving the sea surface temperature. *J. Phys. Oceanogr.,* **22,** 859–881.

Ciasto, L. M., and D. W. J. Thompson, 2004: North Atlantic atmosphere–ocean interaction on intraseasonal time scales. *J. Climate,* **17,** 1617–1621.

Czaja, A., and C. Frankignoul, 2002: Observed impact of North Atlantic SST anomalies on the North Atlantic Oscillation. *J. Climate,* **15,** 606–623.

Deser, C., and M. S. Timlin, 1997: Atmosphere–ocean interaction on weekly timescales in the North Atlantic and Pacific. *J. Climate,* **10,** 393–408.

Fan, L., Z. Liu, and Q. Liu, 2011: Robust GEFA assessment of climate feedback to SST EOF modes. *Adv. Atmos. Sci.,* **28,** 907–912, doi:10.1007/s00376-010-0081-5.

Frankignoul, C., and E. Kestenare, 2002: The surface heat flux feedback. Part I: Estimates from the observations in the Atlantic and the North Pacific. *Climate Dyn.,* **19,** 633–647.

——, and N. Sennechael, 2007: Observed influence of North Pacific SST anomalies on the atmospheric circulation. *J. Climate,* **20,** 592–606.

——, A. Czaja, and B. L'Heveder, 1998: Air–sea feedback in the North Atlantic and surface boundary conditions for ocean models. *J. Climate,* **11,** 2310–2324.

——, E. Kestenare, and J. Mignot, 2002: The surface heat flux feedback. Part II: Direct and indirect estimates in the ECHAM4/OPA8 coupled GCM. *Climate Dyn.,* **19,** 649–655.

Kalnay, E., and Coauthors, 1996: The NCEP/NCAR 40-Year Reanalysis Project. *Bull. Amer. Meteor. Soc.,* **77,** 437–471.

Kelly, K. A., and S. Dong, 2004: The relation of western boundary current heat transport and storage to mid-latitude ocean–atmosphere interaction. *Earth's Climate: The Ocean–Atmosphere Interaction, Geophys. Monogr.,* Vol. 147, Amer. Geophys. Union, 347–363.

Kushnir, Y., and I. M. Held, 1996: Equilibrium atmospheric response to North Atlantic SST anomalies. *J. Climate,* **9,** 1208–1220.

——, W. A. Robinson, I. Bladé, N. M. J. Hall, S. Peng, and R. Sutton, 2002: Atmospheric GCM response to extratropical SST anomalies: Synthesis and evaluation. *J. Climate,* **15,** 2233–2256.

Kwon, Y.-O., M. A. Alexander, N. A. Bond, C. Frankignoul, H. Nakamura, B. Qiu, and L. A. Thompson, 2010: Role of the Gulf Stream and Kuroshio–Oyashio systems in large-scale atmosphere–ocean interaction: A review. *J. Climate,* **23,** 3249–3281.

Latif, M., and T. P. Barnett, 1994: Causes of decadal climate variability in the North Pacific/North American sector. *Science,* **266,** 634–637.

Lau, N.-C., A. Leetmaa, and M. J. Nath, 2006: Attribution of atmospheric variations in the 1997–2003 period to SST anomalies in the Pacific and Indian Ocean basins. *J. Climate,* **19,** 3607–3628.

Liu, Q., N. Wen, and Z. Liu, 2006: An observational study of the impact of the North Pacific SST on the atmosphere. *Geophys. Res. Lett.,* **33,** L18611, doi:10.1029/2006GL026082.

Liu, Z., and L. Wu, 2004: Atmospheric response to North Pacific SST: The role of ocean–atmosphere coupling. *J. Climate,* **17,** 1859–1882.

——, and N. Wen, 2008: On the assessment of nonlocal climate feedback. Part II: EFA-SVD analysis and optimal feedback. *J. Climate,* **21,** 5402–5415.

——, ——, and Y. Liu, 2008: On the assessment of nonlocal climate feedback. Part I: The generalized equilibrium feedback analysis. *J. Climate,* **21,** 134–148.

——, ——, and L. Fan, 2012a: Assessing atmospheric response to surface forcing in the observation. Part I: Cross validation of annual response using GEFA, LIM, and FDT. *J. Climate,* **25,** 6796–6816.

——, L. Fan, S. I. Shin, and Q. Liu, 2012b: Assessing atmospheric response to surface forcing in the observation. Part II: Cross validation of seasonal response using GEFA and LIM. *J. Climate,* **25,** 6817–6834.

Minobe, S., A. Kuwano-Yoshida, N. Komori, S. Xie, and R. J. Small, 2008: Influence of the Gulf Stream on the troposphere. *Nature,* **452,** 206–209.

Nonaka, M., and S. P. Xie, 2003: Covariations of sea surface temperature and wind over the Kuroshio and its extension: Evidence for ocean-to-atmosphere feedback. *J. Climate,* **16,** 1404–1413.

Palmer, T. N., and Z. Sun, 1985: A modeling and observational study of the relationship between sea surface temperature in the north-west Atlantic and the atmospheric general circulation. *Quart. J. Roy. Meteor. Soc.,* **111,** 947–975.

Park, S., C. Deser, and M. A. Alexander, 2005: Estimation of the surface heat flux response to sea surface temperature anomalies over the global oceans. *J. Climate,* **18,** 4582–4599.

Peng, S., L. A. Mysak, H. Richtie, J. Derome, and B. Dugas, 1995: The differences between early and midwinter atmospheric responses to sea surface temperature anomalies in the northwest Atlantic. *J. Climate,* **8,** 137–157.

Rahmstorf, S., and J. Willebrand, 1995: The role of temperature feedback in stabilizing the thermohaline circulation. *J. Phys. Oceanogr.,* **25,** 787–805.

Tanimoto, Y., H. Nakamura, T. Kagimoto, and S. Yamane, 2003: An active role of extratropical sea surface temperature anomalies in determining anomalous turbulent heat fluxes. *J. Geophys. Res.,* **108,** 3304, doi:10.1029/2002JC001750.

Vimont, D. J., D. S. Battisti, and A. C. Hirst, 2001: Footprinting: A seasonal connection between the tropics and midlatitudes. *Geophys. Res. Lett.,* **28,** 3923–3926.

Wen, N., Z. Liu, Q. Liu, and C. Frankignoul, 2005: Observations of SST, heat flux and North Atlantic Ocean–atmosphere interaction. *Geophys. Res. Lett.,* **32,** L24619, doi:10.1029/2005GL024871.

——, ——, ——, and ——, 2010: Observed atmospheric responses to global SST variability modes: A unified assessment using GEFA. *J. Climate,* **23,** 1739–1759.

Zhong, Y., and Z. Liu, 2008: A joint statistical and dynamical assessment of atmospheric response to North Pacific oceanic variability in CCSM3. *J. Climate,* **21,** 6044–6051.

——, ——, and M. Notaro, 2011: A GEFA assessment of global ocean influence on U.S. hydroclimate variability: Attribution to regional SST variability modes. *J. Climate,* **24,** 693–707.